

Dynamical scheme for hadronization with first-order phase transition

Bohao Feng,¹ Zhe Xu ^{*,1} and Carsten Greiner²

¹*Department of Physics, Tsinghua University and Collaborative Innovation Center of Quantum Matter, Beijing 100084, China*

²*Institut für Theoretische Physik, Johann Wolfgang Goethe-Universität Frankfurt, Max-von-Laue-Strasse 1, 60438 Frankfurt am Main, Germany*

We present a dynamical scheme for hadronization with first-order confinement phase transition. The thermodynamical conditions of phase equilibrium, the fluid velocity profile, and the dissipative effect determine the macroscopic changes of the parton volume and the corresponding hadron volume during the phase transition. The macroscopic volume changes are the basis for building up a dynamical scheme by considering microscopic transition processes from partons to hadrons and backwards. The established scheme is proved by comparing the numerical results with the analytical solutions in the case of a one-dimensional expansion of a dissipative fluid with Bjorken boost invariance. The comparisons show almost perfect agreements, which demonstrate the applicability of the introduced scheme.

I. INTRODUCTION

The relativistic heavy-ion collisions provide an opportunity in the laboratory to investigate QCD matter under extreme conditions of high temperature, high density, and strong electromagnetic field. Data taken in experiments at the Relativistic Heavy Ion Collider (RHIC) [1–4] and at the Large Hadron Collider (LHC) [5–7] indicate the transient existence of a quark-gluon plasma (QGP), which then undergoes phase transitions and gradually merges into a large number of hadrons. We are interested in the dynamical process of the phase transition, which is essentially needed, in order to have a complete physical picture of relativistic heavy-ion collisions and to understand phenomena found at RHIC and LHC. In particular, the dynamical description of the phase transition could determine the contribution of gluons in the buildup of the collective flow of hadrons, which has not been intensively studied so far. In quark coalescence models [8], which have been employed to explain the quark number scaling behavior in the hadronic elliptic flows found at RHIC [9], gluons are not explicitly considered.

Another motivation concerns the viscous effect during the phase transition. In viscous hydrodynamical calculations [10–14] the shear viscosity to the entropy density ratio (η/s) of the parton-hadron mixture during the phase transition is set to be constant. However, this treatment is only an assumption, since there is no evidence for the equal η/s of partons and hadrons at the phase transition. The dynamical description of the phase transition would determine the real viscous corrections to the thermal distribution functions of each hadron species [15] and would examine the applicability of the Cooper-Frye prescription [16] used in viscous hydrodynamical calculations.

Since the dynamical description for the phase transition from first principle is at present an unsolved problem, we have to content ourselves with modeling, which allows exploring related phenomena in an articulated

way. In this article we will introduce a dynamical scheme for the confinement phase transition of first order.

The purpose of this article is conceptional. We consider, for simplicity, the transition from gluons to pions. The gluons that we concern are soft particles, which build up the bulk of the medium. We do not discuss the hadronization of gluon jets. Also, we do not discuss the transition from gluons to glueballs [17], which is a sharp first-order phase transition [18]. We *assume* that the hadronization from gluons to pions is a first-order phase transition. Although this contradicts the fact that the QCD transition at zero baryon chemical potential is a crossover [19, 20], the condition of phase equilibrium that keeps the temperature and chemical potential of gluonic and pionic phase equal and constant during the first-order phase transition will prove numerical implementations. Simulating the crossover phase transition needs the correct implementation of the equation of state (EoS) from the lattice QCD calculations and is a future project. The present work can be seen as an attempt to describe a first-order phase transition between two phases with different degrees of freedom. It is the first step towards a full scheme describing the first-order phase transition from quarks and gluons to mesons and baryons at a finite baryonic chemical potential. Adding quarks and more hadron species into the scheme is more complicated, but in line with the present implementation, and will be shown in a forthcoming paper.

The numerical implementation of hadronization that we introduce is a further extension of the existing parton cascade BAMPS (Boltzmann Approach of Multi Parton Scatterings) [21], which describes the pre-equilibrium stage, the thermalization, and the hydrodynamical evolution of quarks and gluons produced in ultrarelativistic heavy-ion collisions. The dynamical hadronization scheme will serve as an interface between BAMPS and hadronic transport model, which will be developed next. BAMPS is a numerical solver of the kinetic Boltzmann equations for on-shell quarks and gluons by using test particles to represent phase space distribution functions of quarks and gluons. Interactions of quarks and gluons are simulated by the stochastic interpretation of the tran-

*xuzhe@mail.tsinghua.edu.cn

sition rates of scattering processes. The numerical implementation of transitions from gluons to pions, which will be presented in this article, has the same means as used in BAMPS for interactions of quarks and gluons. We will show that the effective probabilities of the microscopic processes for transitions from gluons to pions are entirely determined by the thermodynamical feature of the phase transition, the viscosity of the QCD matter, and the velocity profile of the hydrodynamical expansion. Our numerical implementation is different from the hadronization procedures used in transport models such as AMPT (A multiphase transport model) [22], PHSD (Parton-Hadron-String Dynamics) [23], etc.

The article is organized as follows. In Sec. II we derive the volume change of gluons and pions during the phase transition, based on the conditions of phase equilibrium at the first-order phase transition and hydrodynamical equations. With this we establish a dynamical scheme transferring gluon matter to pion matter during the first-order phase transition in Sec. III. In Sec. IV the analytical formulas of the gluonic volume fraction, number, energy, and entropy density are derived in the case of a one-dimensional expansion with Bjorken boost invariance, in order to prove the numerical implementations by comparing the analytical solutions with numerical results shown in Sec. VI. Before doing the comparisons, we present details of numerical implementations and setups in Sec. V. Finally we summarize and give an outlook in Sec. VII.

II. THE EOS AND THE FIRST-ORDER PHASE TRANSITION IN A GLUON-PION MIXTURE

For the EoS of gluons we employ the standard MIT bag model [24]. The pressure and energy density are

$$P_g = \frac{1}{3}(e_g - 4B) = n_g T_g - B, \quad (1)$$

$$e_g = 3n_g T_g + B, \quad (2)$$

where n_g denotes the gluon number density and T_g is the temperature. For the bag constant we use $B^{1/4} = 0.23$ GeV. The pion system is considered as an ideal gas. We neglect pion's rest mass for simplicity. The pressure and energy density of massless pions are then

$$P_\pi = \frac{1}{3}e_\pi = n_\pi T_\pi, \quad (3)$$

$$e_\pi = 3n_\pi T_\pi, \quad (4)$$

where n_π denotes the pion number density and T_π the temperature. Here we have ignored the quantum Bose enhancement [25] of gluons and pions and regarded them as Boltzmann particles.

For the first-order phase transition, both EoS of gluons and pions are matched to each other via the Gibbs condition [26–28],

$$P_g = P_\pi \equiv P_c, \quad T_g = T_\pi \equiv T_c, \quad \mu_g = \mu_\pi \equiv \mu_c. \quad (5)$$

μ_g and μ_π are the chemical potential of gluons and pions, respectively, which are defined by

$$e^{\frac{\mu_i}{T_i}} = \frac{n_i}{n_i^{eq}}, \quad (6)$$

where i stands for g or π . n_i^{eq} is the particle number density in thermal equilibrium,

$$n_i^{eq} = \frac{d_i}{\pi^2} T_i^3, \quad (7)$$

where $d_g = 16$ and $d_\pi = 3$ are the degeneracy factor of gluons and pions, respectively.

Now we consider the confinement phase transition in an expanding QCD matter. Suppose V is the volume of an expanding element in its local rest frame at proper time τ . During the phase transition the volume of pions is increasing, while the volume of gluons is decreasing. We denote V_g and V_π as the volume of gluons and pions. The fraction of the gluon phase to the mixture is then $f_g = V_g/V = V_g/(V_g + V_\pi)$. The total particle number and energy density are

$$n_m = n_g^c f_g + n_\pi^c (1 - f_g), \quad (8)$$

$$e_m = e_g^c f_g + e_\pi^c (1 - f_g), \quad (9)$$

where n_g^c, e_g^c (n_π^c, e_π^c) are the particle number and energy density of gluons (pions) at the transition temperature T_c , respectively. From the above equations for n_m and e_m , and the EoS of gluons and pions it follows

$$e_m + P_c = 4n_m T_c. \quad (10)$$

In the following we derive the time dependence of f_g in a local region under the Gibbs condition (5). In our dynamical scheme gluons hadronize smoothly into pions. We do not consider spinodal instabilities [29], which lead to fluctuations in the baryon density [30, 31], for instance. It would be possible to introduce spinodal instabilities when adding quarks and baryons in our scheme and incorporating the mean field into Vlasov term of the Boltzmann equation.

During a time step $d\tau$ the considered volume element is expanded to $V + dV$. The volume of gluons is decreased to $V_g + dV_g$, while the volume of pions is increased to $V_\pi + dV_\pi$. dV_g is negative. Thus, $dV_\pi = dV - dV_g$ is larger than $-dV_g$. The volume changes indicate that $-n_g^c dV_g$ gluons are confined into $n_\pi^c dV_\pi$ pions and an energy of a amount of $-e_g^c dV_g$ has to be redistributed to the pionic and gluonic phase in order to maintain the Gibbs condition Eq. (5).

For a hydrodynamic system, its energy density changes according to the hydrodynamical equation [32],

$$De = -(e + P)\nabla_\mu U^\mu + \pi^{\mu\nu}\nabla_{<\mu}U_{>\nu}, \quad (11)$$

where U^μ is the fluid four-velocity and $\pi^{\mu\nu}$ is the shear tensor. Symbols in the above equation are defined as

follows:

$$D = U^\mu \partial_\mu, \quad (12)$$

$$\nabla^\mu = \Delta^{\mu\nu} \partial_\nu, \quad (13)$$

$$\Delta^{\mu\nu} = g^{\mu\nu} - U^\mu U^\nu, \quad (14)$$

$$A^{<\mu\nu>} = \left[\frac{1}{2} (\Delta_\sigma^\mu \Delta_\tau^\nu + \Delta_\sigma^\nu \Delta_\tau^\mu) - \frac{1}{3} \Delta^{\mu\nu} \Delta_{\sigma\tau} \right] A^{\sigma\tau} \quad (15)$$

In Eq. (11) the heat transfer is neglected and the bulk pressure is zero, since here we consider systems of massless particles. The right hand side of Eq. (11) can be written as $-(e + P_{eff}) \nabla_\mu U^\mu$ by introducing an effective pressure $P_{eff} = P + \tilde{\pi}$, where

$$\tilde{\pi} = -\frac{\pi^{\mu\nu} \nabla_{<\mu} U_{>\nu}}{\nabla_\mu U^\mu}. \quad (16)$$

For a pure one-component system, the kinetic energy in the rest frame of an expanding volume element decreases by $dE = -P_{eff} dV$ due to the work done by the effective pressure. Thus, the temperature decreases too.

In order to hold the Gibbs condition (5) during the phase transition, there must be energy influxes into the gluonic and pionic phase, which compensate the energy loss of $dE_g = -(P_c + \tilde{\pi}_g) f_g dV$ and $dE_\pi = -(P_c + \tilde{\pi}_\pi)(1 - f_g) dV$ in the gluonic and pionic phase, respectively. All these energies should come from the transition energy $-e_g^c dV_g$. After subtracting dE_g and dE_π from $-e_g^c dV_g$, the remaining energy is the energy of newly produced pions and must be equal to $e_\pi^c dV_\pi$, in order to keep the temperature of pions as T_c . The energy balance reads

$$-e_g^c dV_g - (P_c + \tilde{\pi}_g) f_g dV - (P_c + \tilde{\pi}_\pi)(1 - f_g) dV = e_\pi^c dV_\pi. \quad (17)$$

Inserting the EoS of gluons, Eqs. (1) and (2), into the left-hand side of the energy balance (17) gives

$$\begin{aligned} & -(3n_g^c T_c + B) dV_g - (n_g^c T_c - B + \tilde{\pi}_g) f_g dV \\ & - (P_c + \tilde{\pi}_\pi)(1 - f_g) dV \\ & = -3n_g^c T_c dV_g + B(-dV_g + f_g dV) - (n_g^c T_c + \tilde{\pi}_g) f_g dV \\ & - (P_c + \tilde{\pi}_\pi)(1 - f_g) dV. \end{aligned} \quad (18)$$

The second term on the right-hand side of the above equation, which is proportional to the bag constant, is the latent heat, dE_{lat} , provided by the bag pressure in volume V during time $d\tau$. Then the terms in the energy balance Eq. (17) are rearranged to

$$-3n_g^c T_c dV_g + dE_{lat} = e_\pi^c dV_\pi + (n_g^c T_c + \tilde{\pi}_g) f_g dV + (P_c + \tilde{\pi}_\pi)(1 - f_g) dV. \quad (19)$$

We see that the kinetic energy of hadronizing gluons together with the absorbed latent heat cover the energy of produced pions with T_c and the loss of kinetic energies of gluons and pions due to the work done by the effective pressure.

Putting $dV_\pi = dV - dV_g$ in the energy balance Eq. (17) we obtain

$$dV_g = -\frac{e_\pi^c + P_c + \tilde{\pi}_m}{e_g^c - e_\pi^c} dV \quad (20)$$

with $\tilde{\pi}_m = \tilde{\pi}_g f_g + \tilde{\pi}_\pi(1 - f_g)$. dV can be determined according to the identity

$$\frac{1}{V} \frac{dV}{d\tau} = \nabla_\mu U^\mu. \quad (21)$$

From the definition of f_g and Eqs. (20) and (21), we have

$$\begin{aligned} \frac{df_g}{d\tau} &= \frac{1}{V} \frac{dV_g}{d\tau} - f_g \frac{1}{V} \frac{dV}{d\tau} \\ &= \left[-\frac{e_\pi^c + P_c + \tilde{\pi}_m}{e_g^c - e_\pi^c} - f_g \right] \nabla_\mu U^\mu, \end{aligned} \quad (22)$$

which can be solved to obtain the time dependence of f_g . Once we know U^μ and $\pi^{\mu\nu}$ from transport or hydrodynamic calculations, we can determine dV_g and f_g . In addition, the latent heat can be expressed as

$$dE_{lat} = B(-dV_g + f_g dV) = \frac{e_m + P_c + \tilde{\pi}_m}{e_g^c - e_\pi^c} B dV. \quad (23)$$

We notice that Eq. (20) can be derived in a pure mathematical way. For that we first differentiate the energy density in Eq. (9) with respect to τ and equate this with the hydrodynamical equation (11) to get $df_g/d\tau$. We then use the first identity of Eq. (22) to obtain dV_g , which is found to be identical to Eq. (20). This consistence confirms the correct dynamical picture of the first-order phase transition near equilibrium.

Equation (20) is indeed an important result, which shows quantitatively how the transition between gluons and pions proceeds and is a basic equation for establishing a microscopic transport scheme for the first-order phase transition. Although Eq. (20) has been derived for a transition from gluons to pions in an expanding volume element, it is also valid for a transition from pions to gluons in a contracting volume element, where dV and $\nabla_\mu U^\mu$ are negative. In this case the volume element gains energy from the surrounding medium. The energy balance in Eq. (19) can be reinterpreted that the sum of the energy from the transition $-e_\pi^c dV_\pi$ and that from the surrounding medium $-(n_g^c T_c + \tilde{\pi}_g) f_g dV$ and $-(P_c + \tilde{\pi}_\pi)(1 - f_g) dV$ is equal to the sum of the kinetic energy of newly produced gluons $3n_g^c T_c dV_g$ and the released latent heat $-dE_{lat}$.

From Eq. (20) we see the viscous effect on the phase transition. For a perfect fluid, where $\tilde{\pi}_m = 0$, $|dV_g/dV|$ is a constant, whereas for a viscous fluid $|dV_g/dV|$ is time dependent and is smaller (larger) than that for $\tilde{\pi}_m = 0$ in a transition from gluons to pions (from pions to gluons), since $\tilde{\pi}_m$ is negative (positive) in an expanding (a contracting) system [see Eq. (16)]. The different behavior of $|dV_g/dV|$ in transitions from gluons to pions and backwards is due to the fact that the process of the phase transition with non-zero viscosity is irreversible.

Moreover, in an expanding system $e_\pi^c + P_c + \tilde{\pi}_m$ could be negative for large $|\tilde{\pi}_m|$, so that dV_g would become positive, which cannot describe the phase transition from gluons to pions, where dV_g should be negative. This indicates that for large dissipation the first-order phase transition cannot occur. Quantitative statements about an

upper limit of the shear viscosity will be made elsewhere. We mention that it seems that there is no such upper limit of the shear viscosity for the phase transition from pions to gluons in a contracting system, since $\tilde{\pi}_m$ is positive.

Finally, a nonzero shear viscosity will increase the total entropy during the phase transition. This important feature will be realized in the to be introduced dynamical scheme of hadronization. Before we proceed, the entropy density is given by

$$s_i = \frac{e_i + P_i - \mu_i n_i}{T_i} = \left(4 - \frac{\mu_i}{T_i}\right) n_i, \quad (24)$$

where i stands for g or π . During the phase transition the total entropy density is

$$s_m = s_g^c f_g + s_\pi^c (1 - f_g) = \left(4 - \frac{\mu_c}{T_c}\right) n_m, \quad (25)$$

where s_g^c and s_π^c are the entropy density of gluons and pions at the transition temperature T_c .

III. THE DYNAMICAL SCHEME FOR HADRONIZATION

In the rest of the article we consider only the phase transition from gluons to pions in expanding systems.

Using Eq. (20) we find that the difference between the number of gained pions and the number of lost gluons in the volume element V during $d\tau$ is

$$n_\pi^c dV_\pi - (-n_g^c dV_g) = -\frac{\tilde{\pi}_m}{4T_c} dV, \quad (26)$$

which is non-negative, since $\tilde{\pi}_m \leq 0$ from Eq. (16). This indicates that for an ideal fluid the number of gained pions is the same as that of lost gluons, while for a viscous fluid the number of gained pions is larger than that of lost gluons, which increases the total entropy. Therefore, we in principle need number-changing processes, such as two gluons go to three pions, $g + g \rightarrow \pi + \pi + \pi$, to implement hadronization in a viscous fluid. We will see later that a part of the latent heat provides an additional energy to the three pions, so that the temperature and chemical potential of pions keep constant.

For the phase transition from gluons to pions we consider the following processes: $g + g \rightarrow \pi + \pi + \pi$, $g + g \rightarrow \pi + \pi$, and back reactions $\pi + \pi + \pi \rightarrow g + g$ and $\pi + \pi \rightarrow g + g$. Here we hide the charge of pions, which could be noted explicitly as $g + g \leftrightarrow \pi^+ + \pi^- + \pi^0$, $g + g \leftrightarrow \pi^0 + \pi^0 + \pi^0$, $g + g \leftrightarrow \pi^+ + \pi^-$, and $g + g \leftrightarrow \pi^0 + \pi^0$. The probabilities of the occurrence of these processes could be tuned to obtain the same yield of all kind of pions. We have to note that the consideration of these microscopic processes is not from the first principle but is necessary to realize the macroscopic volume change according to Eq. (20) and to maintain the Gibbs condition

(5). Therefore, in principle one could consider other processes. The processes we have considered are the simplest one can think of.

When gluons hadronize into pions in the process $g + g \rightarrow \pi + \pi + \pi$ and $g + g \rightarrow \pi + \pi$, besides the total kinetic energy of gluons, an amount of energy from the bag pressure (latent heat), will be involved in the total energy of pions. Therefore, the average energy of each produced pion is larger than that of the lost gluons, which is $3T_c$. We denote the ratio of the total energy of the final pions over the total kinetic energy of the initial gluons by x , which is larger than 1. We will show later that the determination of the ratio x [see Eq. (36)] corresponds to the latent heat [see Eq. (23)]. It is obvious that the total kinetic energy is not conserved in the processes $g + g \rightarrow \pi + \pi + \pi$ and $g + g \rightarrow \pi + \pi$. Since transitions with momentum and kinetic energy conservation have been numerically implemented in a standard routine, we *amplify* the momentum (also the kinetic energy) of each gluon by x before performing the transitions to pions by using the standard routine. One can easily prove that the factor x is Lorentz invariant.

Since the latent heat has been involved in $g + g \rightarrow \pi + \pi + \pi$ and $g + g \rightarrow \pi + \pi$ according to Eq. (23), in back reactions $\pi + \pi + \pi \rightarrow g + g$ and $\pi + \pi \rightarrow g + g$ the total momentum as well as the total kinetic energy are conserved. We allow only those back reactions to occur, if pions are newly produced from $g + g \rightarrow \pi + \pi + \pi$ and $g + g \rightarrow \pi + \pi$. Thus, on average, each gluon coming from back reactions has a larger energy than $3T_c$. This mimics the energy transfer from the pionic phase to the gluonic phase, in order to compensate for the energy loss of gluons due to the hydrodynamical expansion. We involve back reactions in processes $g + g \rightarrow \pi + \pi + \pi \rightarrow g^* + g^*$, $g + g \rightarrow \pi + \pi + \pi \rightarrow g^* + g^* + \pi$, and $g + g \rightarrow \pi + \pi \rightarrow g^* + g^*$, where three pions or two pions are regarded as intermediate states and g^* denotes outgoing gluons with a higher averaged energy than that of initial gluons. Numerically we implement $g + g \rightarrow g^* + g^*$ and $g + g \rightarrow g^* + g^* + \pi$ directly and do not specify intermediate states explicitly.

Now we derive the probability that a process $g + g \rightarrow \pi + \pi + \pi$, $g + g \rightarrow \pi + \pi$, $g + g \rightarrow g^* + g^* + \pi$, or $g + g \rightarrow g^* + g^*$ occurs, denoted by P_{23} , P_{22} , P_{23b} , and P_{22b} , respectively. For simplicity, these probabilities are assumed to be independent on the momenta of particles involved in the processes. Therefore, the number of lost gluons and gained pions in volume V during $d\tau$ relate to the probabilities P_{23} , P_{22} , and P_{23b} as follows:

$$\frac{1}{2} N_g (N_g - 1) (2P_{23} + 2P_{22}) = -n_g^c dV_g, \quad (27)$$

$$\frac{1}{2} N_g (N_g - 1) (3P_{23} + 2P_{22} + P_{23b}) = n_\pi^c dV_\pi, \quad (28)$$

where $N_g = n_g^c V$ is the gluon number in volume V . Suppose the number of g^* from the back reactions is

dN_{g^*} ; then we have

$$\frac{1}{2}N_g(N_g - 1)(2P_{23b} + 2P_{22b}) = dN_{g^*}. \quad (29)$$

The total kinetic energy of initial gluons in each transition process is $6T_c$ ($3T_c$ for each) on average. As introduced before, we enhance the kinetic energy of initial gluons by a x factor, in order to include the latent heat. The total energy involved in each transition process is then $6T_c x$ on average, while the latent heat per process is $6T_c(x - 1)$. The total involved latent heat in volume V during $d\tau$ relates to the sum of the probabilities of all the transition processes as well as the factor x ,

$$\begin{aligned} & \frac{1}{2}N_g(N_g - 1)(P_{23} + P_{22} + P_{23b} + P_{22b})6T_c(x - 1) \\ &= dE_{lat} = \frac{e_m + P_c + \tilde{\pi}_m}{e_g^c - e_\pi^c} B dV. \end{aligned} \quad (30)$$

The second identity is due to Eq. (23).

In the process $g + g \rightarrow \pi + \pi$ the energy of each pion is $3T_c x$ on average, while it is $2T_c x$ in the processes $g + g \rightarrow \pi + \pi + \pi$ and $g + g \rightarrow g^* + g^* + \pi$. The average energy of each pion obtained from $g + g \rightarrow \pi + \pi$, $g + g \rightarrow \pi + \pi + \pi$, and $g + g \rightarrow g^* + g^* + \pi$ should be larger than $3T_c$. In other words, the total energy of these pions should be larger than $3T_c n_\pi^c dV_\pi = e_\pi^c dV_\pi$, because the energy excess over $e_\pi^c dV_\pi$ should cover the energy loss of all pions in volume V due to the work done by the effective pressure. This requirement leads to

$$\begin{aligned} & \frac{1}{2}N_g(N_g - 1) \left(P_{23} + P_{22} + \frac{1}{3}P_{23b} \right) 6T_c x \\ &= e_\pi^c dV_\pi + (n_\pi^c T_c + \tilde{\pi}_\pi)(1 - f_g) dV. \end{aligned} \quad (31)$$

Analogously, the total energy of the gained gluons in the processes $g + g \rightarrow g^* + g^*$ and $g + g \rightarrow g^* + g^* + \pi$ should be larger than $3T_c dN_{g^*}$, because the excess should cover the energy loss of all gluons in volume V due to the work done by the kinetic pressure, which leads to

$$\begin{aligned} & \frac{1}{2}N_g(N_g - 1) \left(P_{22b} + \frac{2}{3}P_{23b} \right) 6T_c x \\ &= 3T_c dN_{g^*} + (n_g^c T_c + \tilde{\pi}_g) f_g dV. \end{aligned} \quad (32)$$

We eliminate dN_{g^*} by inserting Eq. (29) and obtain

$$\begin{aligned} & \frac{1}{2}N_g(N_g - 1) \left[P_{22b}(x - 1) + P_{23b} \left(\frac{2}{3}x - 1 \right) \right] 6T_c \\ &= (n_g^c T_c + \tilde{\pi}_g) f_g dV. \end{aligned} \quad (33)$$

We notice that Eq. (33) plus Eq. (31) minus $3T_c$ times Eq. (27) is equal to Eq. (30) by using the energy balance Eq. (19). This indicates that there are only four independent equations, Eqs. (27), (28), (31), and (33), available for five unknowns, namely, four probabilities P_{23} , P_{22} , P_{23b} , P_{22b} , and the factor x . One of five unknowns is a free parameter. The determination of this free parameter

should ensure that all the probabilities are non-negative and x is larger than 1. We choose P_{23} as the free parameter and set it to be zero. With this choice all other transition probabilities are positive and the factor x is larger than 1, as shown later in Fig. 3. $P_{23} = 0$ does not mean that there are no $g + g \rightarrow \pi + \pi + \pi$ processes, but indicates that once such a process occurs, either three or two pions will go back to two gluons, which are denoted by the processes $g + g \rightarrow \pi + \pi + \pi \rightarrow g^* + g^*$ or $g + g \rightarrow \pi + \pi + \pi \rightarrow g^* + g^* + \pi$.

With $P_{23} = 0$ we obtain P_{22} directly from Eq. (27)

$$\begin{aligned} P_{22} &= -\frac{n_g^c dV_g}{N_g(N_g - 1)} \\ &= \frac{n_g^c(e_\pi^c + P_c + \tilde{\pi}_m)}{e_g^c - e_\pi^c} \frac{dV}{N_g(N_g - 1)} \\ &= \frac{n_g^c(e_\pi^c + P_c + \tilde{\pi}_m)}{e_g^c - e_\pi^c} \frac{\nabla_\mu U^\mu V d\tau}{N_g(N_g - 1)} \end{aligned} \quad (34)$$

by using Eqs. (20) and (21). Subtracting Eq. (27) from Eq. (28) gives

$$\begin{aligned} P_{23b} &= \frac{2}{N_g(N_g - 1)} (n_\pi^c dV_\pi + n_g^c dV_g) \\ &= -\frac{\tilde{\pi}_m}{2T_c} \frac{\nabla_\mu U^\mu V d\tau}{N_g(N_g - 1)}. \end{aligned} \quad (35)$$

To get the second identity we have used Eqs. (26) and (21). Putting P_{23b} and P_{22} into Eq. (31) we obtain

$$x = \frac{e_\pi^c dV_\pi + (n_\pi^c T_c + \tilde{\pi}_\pi)(1 - f_g) dV}{T_c(2n_\pi^c dV_\pi - n_g^c dV_g)}, \quad (36)$$

where one may insert the ratios dV_g/dV and $dV_\pi/dV = 1 - dV_g/dV$ from Eq. (20). Finally we get P_{22b} from Eq. (33),

$$P_{22b} = \frac{(n_g^c T_c + \tilde{\pi}_g) f_g + (x - \frac{3}{2}) \tilde{\pi}_m}{3T_c(x - 1)} \frac{\nabla_\mu U^\mu V d\tau}{N_g(N_g - 1)}. \quad (37)$$

With the derived probabilities P_{22} , P_{23b} , P_{22b} , and the factor x , we can perform the corresponding transition processes stochastically in the same manner introduced in BAMPS [21].

For the phase transition from pions to gluons in contracting systems we can analogously consider processes $\pi + \pi \rightarrow g + g$, $\pi + \pi \rightarrow \pi^* + \pi^* + g$, and $\pi + \pi \rightarrow \pi^* + \pi^*$. The factor x is in this case smaller than 1, because a latent heat will be released. The procedure of deriving the probabilities and x is same as that shown above.

Since U^μ and $\pi^{\mu\nu}$ can be extracted from the particle distributions in transport calculations, our dynamical scheme for hadronization with the first-order phase transition can in principle be applied for any systems. In this article we will show a simulation in a particular case, where we consider one-dimensional expansion with Bjorken boost invariance [33], which is widely used to describe the space-time evolution of matter produced

in ultrarelativistic heavy-ion collisions. In this case the time evolution of the phase transition can be calculated analytically, which we use to examine our numerical implementations.

IV. THE CASE OF ONE-DIMENSIONAL EXPANSION WITH BJORKEN BOOST INVARIANCE

In one-dimensional expansion with Bjorken boost invariance, the hydrodynamical velocity is

$$U^\mu = \frac{1}{\tau}(t, 0, 0, z). \quad (38)$$

In the first-order theory of hydrodynamics, the shear tensor reads

$$\pi^{\mu\nu} = 2\eta\nabla^{<\mu}U^{\nu>}, \quad (39)$$

where η is the shear viscosity. Then Eqs. (21), (16), and (11) are reduced to

$$\frac{1}{V} \frac{dV}{d\tau} = \nabla_\mu U^\mu = \frac{1}{\tau}, \quad (40)$$

$$\tilde{\pi} = -2\eta \frac{\nabla^{<\mu}U^{\nu>\nabla_{<\mu}U_{\nu>}}{\nabla_\mu U^\mu} = -\frac{4\eta}{3\tau}, \quad (41)$$

$$\frac{de}{d\tau} = -\frac{e+P}{\tau} + \frac{4\eta}{3\tau^2}. \quad (42)$$

Using Eqs. (25), (10), and (42) we obtain the differential equation for the time evolution of the entropy density during the phase transition

$$\begin{aligned} \frac{ds_m}{d\tau} &= \left(4 - \frac{\mu_c}{T_c}\right) \frac{dn_m}{d\tau} = \left(4 - \frac{\mu_c}{T_c}\right) \frac{1}{4T_c} \frac{de_m}{d\tau} \\ &= -\frac{s_m}{\tau} + \left(1 - \frac{\mu_c}{4T_c}\right) \frac{4\eta_m}{3T_c\tau^2} \end{aligned} \quad (43)$$

with $\eta_m = \eta_g f_g + \eta_\pi(1 - f_g)$. η_g (η_π) is the shear viscosity of gluons (pions). Assuming that η_m/s_m is a constant during the phase transition, we solve Eq. (43) and obtain

$$s_m(\tau) = s_g^c \frac{\tau_c}{\tau} e^{\frac{4a}{3T_c}(\frac{1}{\tau_c} - \frac{1}{\tau})}, \quad (44)$$

where τ_c is the time when the phase transition begins and $a = (1 - \mu_c/4T_c)\eta_m/s_m$. Thus, we get the gluonic fraction in the mixture according to Eq. (25),

$$f_g(\tau) = \frac{s_m(\tau) - s_\pi^c}{s_g^c - s_\pi^c}. \quad (45)$$

f_g decreases from 1 at τ_c to 0 at τ_e , which denotes the time when the phase transition in the considered volume element is complete. In addition, using Eqs. (25) and (10) we have

$$n_m(\tau) = n_g^c \frac{\tau_c}{\tau} e^{\frac{4a}{3T_c}(\frac{1}{\tau_c} - \frac{1}{\tau})}, \quad (46)$$

$$e_m(\tau) = (e_g^c + P_c) \frac{\tau_c}{\tau} e^{\frac{4a}{3T_c}(\frac{1}{\tau_c} - \frac{1}{\tau})} - P_c. \quad (47)$$

V. NUMERICAL IMPLEMENTATIONS AND SETUPS

In this section we give details on numerical implementations and setups for simulating the hadronization in a one-dimensional Bjorken expansion. Since the main goal of this work is to present a dynamical scheme of hadronization and to prove its applicability by comparing the numerical results with analytical solutions, we consider only elastic scatterings among gluons or pions and assume constant cross sections and the isotropic distribution of collision angles. Under these assumptions we can easily tune the cross sections to have a constant η_m/s_m ratio, which is required to obtain analytical solutions; see Eqs. (44) - (47).

Elastic collisions among gluons or pions are simulated by employing the standard BAMPS prescription. The collision probabilities [21] read

$$P_i = v_{rel.} \frac{\sigma_i}{N_{test}} \frac{\Delta t}{f_i V_r}, \quad (48)$$

where i stands for either a process $g + g \rightarrow g + g$ or for $\pi + \pi \rightarrow \pi + \pi$, and σ_i is the respective cross section. $v_{rel.}$ denotes the relative velocity of two incoming particles, and V_r is the volume of a cell in the computational frame. (Remember that V is the cell volume in its local rest frame.) f_i is the gluon or pion fraction, which is f_g or $(1 - f_g)$. Δt is the time step in the computational frame, and N_{test} is the number of test particles per a real particle.

For the isotropic distribution of collision angles the shear viscosity turns out to be [34–36]

$$\eta_i = \frac{6T_i}{5\sigma_i}. \quad (49)$$

Then we can solve Eq. (42) and obtain the time evolution of the energy density of gluons before the phase transition and that for pions after the phase transition:

$$e_g(\tau) = [e_g(\tau_0) - B] \left(\frac{\tau_0}{\tau}\right)^{r_g} + B, \quad (50)$$

$$e_\pi(\tau) = e_\pi(\tau_e) \left(\frac{\tau_e}{\tau}\right)^{r_\pi}, \quad (51)$$

where τ_0 is the initial time of the gluonic phase, and r_g and r_π are given by

$$r_g = \frac{4}{3} - \frac{8}{15n_g(\tau_0)\tau_0\sigma_g}, \quad (52)$$

$$r_\pi = \frac{4}{3} - \frac{8}{15n_\pi(\tau_e)\tau_e\sigma_\pi}. \quad (53)$$

For completeness we give the solutions of the time evolution of number density and temperature, which is defined by the ratio of the kinetic energy density over three-fold of the number density,

$$n_g(\tau) = n_g(\tau_0) \frac{\tau_0}{\tau}, \quad n_\pi(\tau) = n_\pi(\tau_e) \frac{\tau_e}{\tau}, \quad (54)$$

$$T_g(\tau) = T_g(\tau_0) \left(\frac{\tau_0}{\tau}\right)^{r_g-1}, \quad T_\pi(\tau) = T_\pi(\tau_e) \left(\frac{\tau_e}{\tau}\right)^{r_\pi-1} \quad (55)$$

From these results we obtain the time evolution of the chemical potential from Eq. (6). We find that before the phase transition

$$e^{\frac{\mu_g}{T_g}} = e^{\frac{\mu_g(\tau_0)}{T_g(\tau_0)}} \left[\frac{T_g}{T_g(\tau_0)} \right]^{\frac{1}{r_g-1}-3}, \quad (56)$$

which indicates that for nonzero shear viscosity, μ_g will decrease to be negative during expansion, even if the initial state is in thermal equilibrium with $\mu_g(\tau_0) = 0$. Putting the above relation (56) into the Gibbs condition (5) when the phase transition occurs

$$\begin{aligned} P_g &= n_g^c T_c - B = e^{\frac{\mu_c}{T_c}} d_g \frac{T_c^4}{\pi^2} - B \\ &= P_\pi = n_\pi^c T_c = e^{\frac{\mu_c}{T_c}} d_\pi \frac{T_c^4}{\pi^2}, \end{aligned} \quad (57)$$

we get the transition temperature

$$T_c = \left\{ e^{-\frac{\mu_g(\tau_0)}{T_g(\tau_0)}} [T_g(\tau_0)]^{\frac{1}{r_g-1}-3} \frac{\pi^2 B}{d_g - d_\pi} \right\}^{1-\frac{1}{r_g}}. \quad (58)$$

The chemical potential at the transition temperature, μ_c , can be obtained from Eq. (56). The dependence of T_c on the initial state is due to the assumption of the gluon number conservation, which is only valid if the elastic scatterings are dominant processes. On the other hand, if inelastic interactions such like $g + g \leftrightarrow g + g + g$ are as important as the elastic scatterings, the system will go towards chemical equilibrium, i.e., $\mu_g \rightarrow 0$. The dependence of T_c on the initial state will be almost washed out. Since it is easier to obtain analytical solutions when considering elastic collisions only, we do not include inelastic scatterings in the gluonic (and pionic) phase.

Using $T_g(\tau)$ from Eq. (55) and the value of T_c , we obtain the time τ_c , when the phase transition begins

$$\tau_c = \tau_0 \left[\frac{T_g(\tau_0)}{T_c} \right]^{1/(r_g-1)}. \quad (59)$$

Since the time evolutions of the shear viscosity and the entropy density [see Eq. (24)] are known for a chosen constant cross section σ_g , the shear viscosity to the entropy density ratio at τ_c relates to σ_g as

$$\frac{\eta_g(\tau_c)}{s_g(\tau_c)} = \frac{6(d_g - d_\pi)}{5d_g} \frac{T_c^2}{\sigma_g B} \frac{1}{4 - \frac{\mu_g(\tau_0)}{T_g(\tau_0)} - \frac{4-3r_g}{r_g-1} \ln \frac{T_c}{T_g(\tau_0)}}. \quad (60)$$

We have assumed that η_m/s_m is constant during the phase transition. Therefore, $\eta_m/s_m = \text{const.} = \eta_g(\tau_c)/s_g(\tau_c)$. We assume further that the shear viscosity to the entropy density ratio of the gluonic phase is same as that of the pionic phase in the mixture. We have then $\eta_g^c/s_g^c = \eta_\pi^c/s_\pi^c = \text{const.} = \eta_m/s_m$. From Eq. (49) the cross section of pionic scatterings relates to the cross section of gluonic scatterings as

$$\sigma_\pi = \frac{s_g^c}{s_\pi^c} \sigma_g = \frac{d_g}{d_\pi} \sigma_g. \quad (61)$$

We note that the present transport implementation of hadronization with constant η_m/s_m would be equivalent to a hydrodynamic description. The distribution of hadrons after the dynamic hadronization would be almost the same as that obtained by using the Cooper-Frye prescription [16], which switches from viscous hydrodynamic models to hadron transport models [10–14]. However, the assumption of constant η_m/s_m made in this article is only for the comparisons with analytical solutions. In reality the hadronic shear viscosity to the entropy density ratio may be different from the partonic one, which leads to a time-dependent η_m/s_m . The present dynamical scheme of hadronization provides a possibility to examine the applicability of the Cooper-Frye prescription.

In simulations the initial distribution of gluons at τ_0 is assumed to be thermal and boost invariant,

$$f(x, p) = e^{-\frac{p^\mu U_\mu}{T_g}} \bigg|_{\tau_0} = e^{-\frac{p_\perp \cosh(\bar{\eta}-y)}{T_g(\tau_0)}}, \quad (62)$$

where p_\perp is the transverse momentum and $\bar{\eta}$ and y are space-time and momentum rapidity, respectively,

$$\bar{\eta} = \frac{1}{2} \ln \frac{t+z}{t-z}, \quad (63)$$

$$y = \frac{1}{2} \ln \frac{E+p_z}{E-p_z}. \quad (64)$$

We consider gluons between a space-time rapidity window $[-\bar{\eta}_M, \bar{\eta}_M]$ with $\bar{\eta}_M = 3$. Particles are embedded in a three-dimensional box. The transverse plane is a 3×3 fm square. We use periodical boundary condition to cancel the transverse expansion. The longitudinal length of the box is set to be long enough that no particles can exceed the longitudinal bounders at the final time of observation. The box is equidistantly divided into cells with the same transverse length $\Delta x = \Delta y$ and the same distance in the space-time rapidity $\Delta \bar{\eta}$. In simulations we set $\Delta x = \Delta y = 0.25$ fm and $\Delta \bar{\eta} = 0.025$. To avoid numerical artifacts we use a large value of test particle number, $N_{\text{test}} = 14000$.

In the following we show how to extract the volume fraction, particle number and energy density, temperature, and chemical potential of gluons and pions from the numerical simulation. The particle four-flow and the momentum-energy tensor in a transverse slice within $\Delta \bar{\eta}$ are calculated by

$$N^\mu = \int \frac{d^3 p}{(2\pi)^3} \frac{p^\mu}{p^0} f = \frac{1}{V_{\text{slice}}} \frac{1}{N_{\text{test}}} \sum_i \frac{p_i^\mu}{p_i^0}, \quad (65)$$

$$T^{\mu\nu} = \int \frac{d^3 p}{(2\pi)^3} \frac{p^\mu p^\nu}{p^0} f = \frac{1}{V_{\text{slice}}} \frac{1}{N_{\text{test}}} \sum_i \frac{p_i^\mu p_i^\nu}{p_i^0} \quad (66)$$

where the sums are either over gluons or over pions. From N_g^μ for gluons and N_π^μ for pions we calculate the flow velocity U^μ by using the Eckard's definition,

$$U^\mu = \frac{N_g^\mu + N_\pi^\mu}{\sqrt{(N_g^\nu + N_\pi^\nu)(N_{g\nu} + N_{\pi\nu})}}. \quad (67)$$

Then we obtain the particle number and kinetic energy densities in the volume V_{slice}

$$n'_i = N'_i U_\mu, \quad (68)$$

$$e'_i = U_\mu T_i^{\mu\nu} U_\nu, \quad (69)$$

where i stands for gluons or pions. The actual densities of gluons and pions are

$$n_g = n'_g/f_g, \quad e_g = e'_g/f_g + B, \quad (70)$$

$$n_\pi = n'_\pi/(1-f_g), \quad e_\pi = e'_\pi/(1-f_g). \quad (71)$$

We get the temperature of each phases by

$$T_g = \frac{e_g - B}{3n_g} = \frac{e'_g}{3n'_g}, \quad T_\pi = \frac{e_\pi}{3n_\pi} = \frac{e'_\pi}{3n'_\pi}. \quad (72)$$

Since from n'_i and e'_i we cannot uniquely determine μ_g , μ_π , and f_g in the mixture, we assume that $\mu_g/T_g = \mu_\pi/T_\pi$. Thus,

$$\frac{n'_g}{n'_\pi} = \frac{f_g n_g}{(1-f_g)n_\pi} = \frac{f_g}{1-f_g} \frac{n_g^{eq}}{n_\pi^{eq}} = \frac{f_g}{1-f_g} \frac{d_g T_g^3}{d_\pi T_\pi^3} \quad (73)$$

and

$$f_g(\tau) = \left(1 + \frac{d_g T_g^3}{d_\pi T_\pi^3} \frac{n'_\pi}{n'_g} \right)^{-1}. \quad (74)$$

We then have n_g , e_g , n_π , and e_π ; see Eqs. (70) and (71). From these densities we obtain μ_g and μ_π according to their definitions (6).

VI. NUMERICAL RESULTS

In this section we simulate the phase transition from gluons to pions in a one-dimensional expansion with Bjorken boost invariance by implementing the microscopic processes into the parton cascade model BAMPS. We will show the numerical results and compare them with the analytical solutions derived in Secs. IV and V.

As an example, we set the temperature of gluons to be $T_g = 0.3$ GeV at the initial time $\tau_0 = 0.5$ fm/c. Since we will compare the numerical results with the solutions from first-order viscous hydrodynamics, the total cross section of gluon elastic scatterings is set to be a large value of $\sigma_g = 16.5$ mb, which leads to a small shear viscosity to the entropy ratio at the phase transition. With these setups we obtain $T_c = 0.2357$ GeV and $\tau_c = 1.4979$ fm/c from Eqs. (58) and (59). Further we get $\mu_c/T_c = -0.3735$ and $\eta_g/s_g = 0.1045$ at τ_c from Eqs. (56) and (60). In the following we concentrate on the local region at zero space-time rapidity with a small interval of 0.025, and calculate densities in this region.

In the numerical calculation we determine τ_c as follows. According to Eqs. (1), (3), and (5) we have $B = (n_g^c - n_\pi^c)T_c$ at the phase transition. With $n_\pi = n_g d_\pi/d_g$,

which is only true during the phase transition, we see that before the phase transition $(1 - d_\pi/d_g)n_g T_g$ is always larger than B . Therefore, we get τ_c , once

$$\left(1 - \frac{d_\pi}{d_g} \right) n_g(\tau_c) T_g(\tau_c) < B \quad (75)$$

due to numerical fluctuations at the phase transition. From the simulation we extract $\tau_c = 1.4386$ fm/c and accordingly $T_c = 0.2269$ GeV, which slightly differ from the values expected. Although fluctuations exist in numerical extractions of τ_c and T_c , the differences from the expected values have an additional origin. Figure 1 shows the time evolution of the number and kinetic energy density and the temperature of gluons from the initial time τ_0 to the time shortly after τ_c . We have also depicted the analytical solutions from Eqs. (54), (50), and (55) by dashed curves. We see a perfect agreement in the number density n_g , as it should be, since we considered only elastic scatterings of gluons and the time evolution of n_g

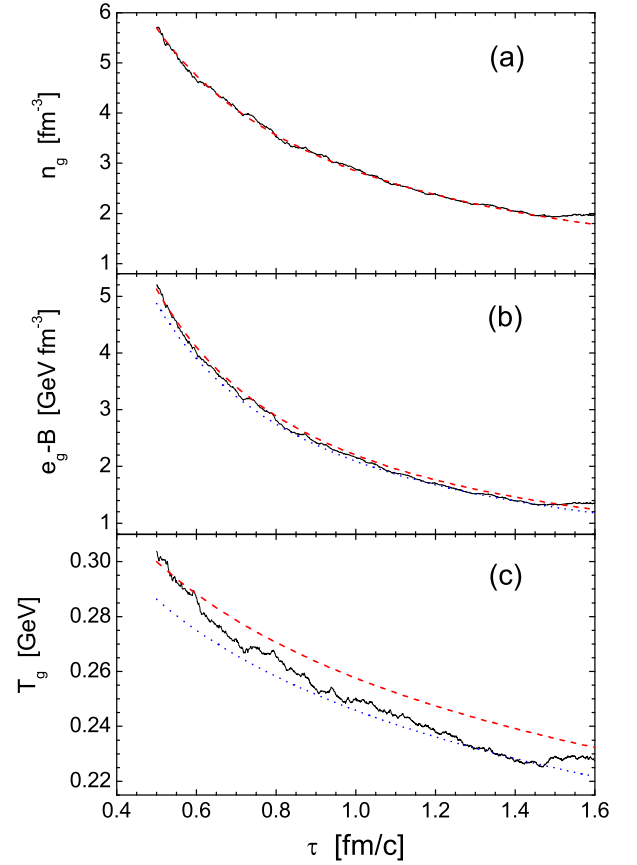


FIG. 1: (Color online) The time evolution of the number and kinetic energy density and the temperature of gluons from $\tau_0 = 0.5$ fm/c to the time shortly after $\tau_c = 1.4386$ fm/c. The numerical results are depicted by solid curves (in black), while the analytical solutions are shown by the dashed curves (in red). The dotted curves (in blue) correspond to the shift of the analytical curves down to meet the values of e_g and T_g at τ_c .

does not depend on the value of the total cross section. On the contrary, deviations are visible in the kinetic energy density $e_g - B$ and in the temperature. We shift the analytical curves down to meet the numerical values of e_g and T_g at τ_c , which correspond to replacing τ_0 by τ_c in Eqs. (50) and (55). The shifted curves are depicted by the dotted curves in Fig. 1. We see agreements between the shifted curves and the numerical results from about 1.2 fm/c to τ_c . Between τ_0 and 1.2 fm/c we see a relaxation from the thermal initial condition to the Navier-Stokes state, which has to be described by second-order or higher order viscous hydrodynamics [32, 37].

From the simulation we get $\eta_g/s_g = 0.1004$ at τ_c , which is slightly different from the expected value, but agrees with the value, when we use the shifted curves in Fig. 1; i.e., we change $T_g(\tau_0)$ and $\mu_g(\tau_0)$ in Eq. (60) accordingly.

We set $n_g^c = n_g(\tau_c)$, $e_g^c = e_g(\tau_c)$, $s_g^c = s_g(\tau_c)$, $\mu_c = \mu_g(\tau_c)$, $\eta_m/s_m = \eta_g(\tau_c)/s_g(\tau_c)$, $n_\pi^c = n_g^c d_\pi/d_g$, $e_\pi^c = (e_g^c - B)d_\pi/d_g$, and $s_\pi^c = s_g^c d_\pi/d_g$. With these densities extracted at τ_c , the gluon fraction f_g extracted at τ , and the gluon number N_g extracted at τ in each cell we compute all the transition probabilities and the factor x at τ according to Eqs. (34), (35), (37), and (36). Here we employ Eqs. (40) and (41) to calculate $\nabla_\mu U^\mu$, $\tilde{\pi}_g$, and $\tilde{\pi}_\pi$ instead of direct extractions from the particle distributions, in order to avoid numerical uncertainties, which could be reduced by using larger N_{test} . In addition, since N_g is proportional to N_{test} and the transition probability should be inversely proportional to N_{test} similar to the collision probability in Eq. (48), we multiply all the transition probabilities by N_{test} .

The actual values of n_g , e_g , n_π , and e_π at τ , calculated by using Eqs. (74), (70), and (71), possess numerical fluctuations, which induce fluctuations in T_g , T_π , μ_g , μ_π , s_g , and s_π , as seen later in Fig. 5. To ensure η_g/s_g and η_π/s_π in the mixture to be equal to η_g/s_g at τ_c , we

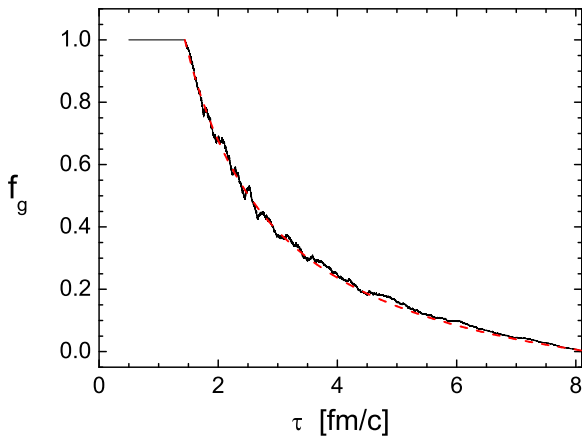


FIG. 2: (Color online) The time evolution of the gluon fraction. The solid curve (in black) depicts the numerical result, while the dashed curve (in red) depicts the expected function.

determine the gluonic (pionic) elastic cross section by

$$\sigma_i(\tau) = \frac{6T_i(\tau)}{5s_i(\tau)} \left[\frac{\eta_g(\tau_c)}{s_g(\tau_c)} \right]^{-1} \quad (76)$$

with $i = g, \pi$ according to Eq. (49). We find (not shown) that the cross sections during the phase transition fluctuate around the given constant values in the pure gluonic or pionic phase.

In Fig. 2 we compare the numerical extracted gluon fraction f_g [according to Eq. (74)] with the expected function [according to Eqs. (44) and (45)] and see a perfect agreement. With the expected function f_g we find the time $\tau_e = 8.233$ fm/c when the hadronization finishes in the considered volume element. Numerically we define τ_e , when on average, the gluon number in a cell is less than two. We find $\tau_e = 8.055$ fm/c, which is slightly earlier than expected. At τ_e there are still few gluons left (about 1% of initial gluons), because one gluon in a cell cannot find another gluon to hadronize. Our numerical handling is as follows: At τ_e we just rename the left gluons to pions without any other changes.

Analogously to the relation between the collision probability and the cross section in Eq. (48), we define the transition cross sections of the processes $g + g \rightarrow \pi + \pi$, $g + g \rightarrow g^* + g^* + \pi$, and $g + g \rightarrow g^* + g^*$ from their transition probabilities. Figure 3 shows the time evolution

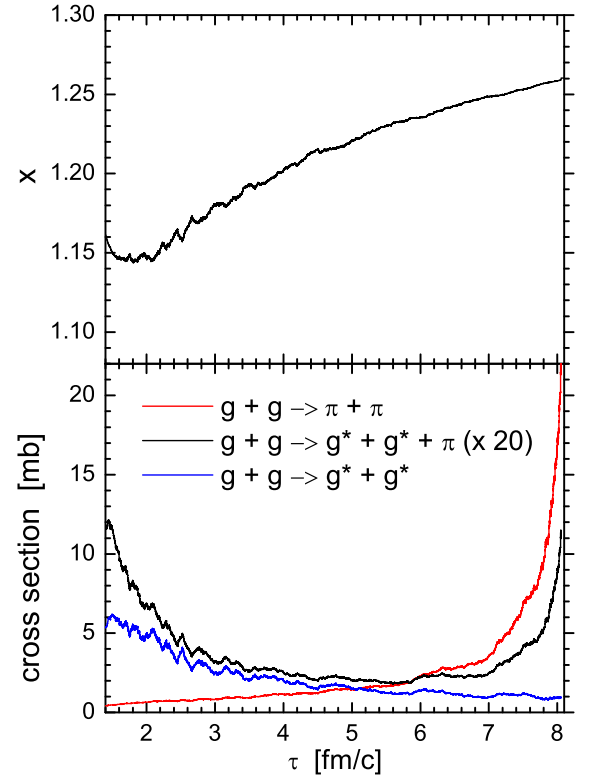


FIG. 3: (Color online) The time evolution of the mean transition cross sections and the factor x .

tion of the mean transition cross sections and the factor x during the phase transition. The cross section of $g + g \rightarrow g^* + g^* + \pi$ is multiplied by 20 and is negligible small due to the small value of η_m/s_m . During the phase transition all cross sections are below 6 mb except for the cross section of $g + g \rightarrow \pi + \pi$ within 0.5 fm/c before the end of the phase transition, which increases into infinity. The divergence happens, because shortly before the complete hadronization the number of gluons is approaching to zero and on the other hand, the hadronization has an approximately constant rate, i.e., $-dV_g \sim Ad\tau$, where A is the transverse area.

Figures 4(a) and 4(b) show the time evolution of the number and the kinetic energy density of gluons (black curves) and pions (red curves), respectively, evaluated according to Eqs. (70), (71), and (74). For comparisons, the densities of pions are multiplied by the ratio of the degeneracy factors d_g/d_π . We see good agreements between the gluonic densities and the amplified pionic densities. We also see that the densities maintain almost constant during the phase transition, expect for larger statistical uncertainties of pionic densities after τ_c and those of gluonic densities before τ_e due to the small amount of particles. Both the average values of the gluon number density and the kinetic energy den-

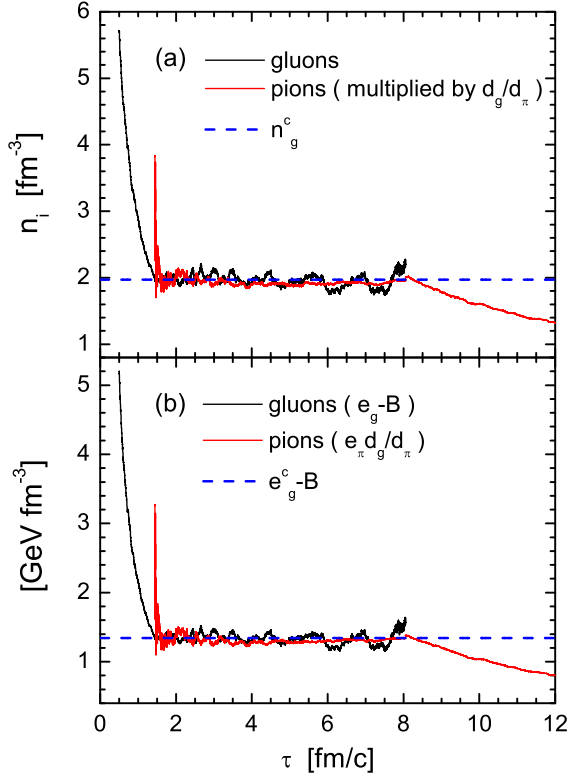


FIG. 4: (Color online) The time evolution of the number and the kinetic energy density. The black (red) curves are for gluons (pions). The dashed lines depict the values at τ_c . From $\tau_e = 8.055$ fm/c, the densities of gluons are zero (not plotted).

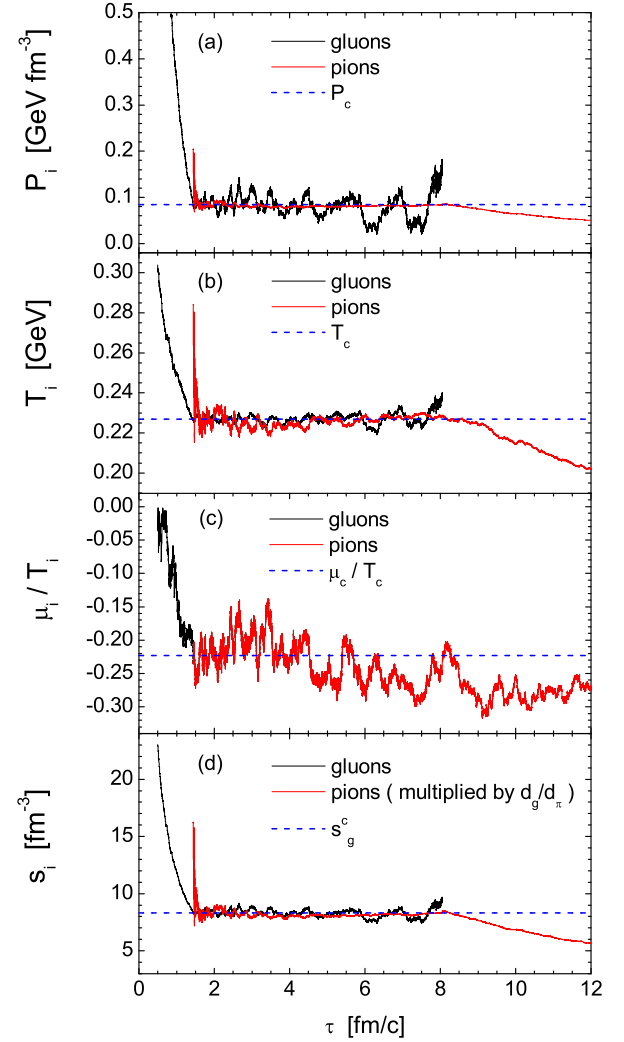


FIG. 5: (Color online) Same as Fig. 4. From top to bottom: The time evolution of the pressure, the temperature, the chemical potential to the temperature ratio, and the entropy density.

sity agree well with $n_g^c = n_g(\tau_c) = 1.9724 \text{ fm}^{-3}$ and $e_g^c - B = e_g(\tau_c) - B = 1.3427 \text{ GeV fm}^{-3}$, which are denoted by the dashed lines.

In Fig. 5 we present the time evolution of the pressure, temperature, chemical potential, and entropy density, which are obtained from the number and energy densities shown in Fig. 4. Figure 5(a) pictures the pressure of gluons and pions, which are obtained according to the equations of state Eqs. (1) and (3). The temperatures are calculated from Eq. (72) and shown in Fig. 5(b). We see that the pressures and temperatures are almost constant during the phase transition. The average values also agree well with $P_c = P_g(\tau_c) = 0.0834 \text{ GeV fm}^{-3}$ and $T_c = T_g(\tau_c) = 0.2269 \text{ GeV}$, which are denoted by the dashed lines. From the number and the kinetic energy density we also obtain the chemical potential of gluons and pions according to the definition (6). In Fig.

5(c) we plot the time evolution of the ratio of the chemical potential to the temperature. μ_g/T_g is exactly the same as μ_π/T_π during the phase transition, because this is the assumption for extracting f_g [see Eq. (74)]. We see that μ_g/T_g (also μ_π/T_π) is almost constant around $\mu_c/T_c = \mu_g(\tau_c)/T_g(\tau_c) = -0.223$. We have demonstrated that the Gibbs condition (5) is realized in our numerical implementations. Finally we show in Fig. 5(d) the time evolution of the entropy density of gluons and pions obtained according to Eq. (24). Same as the number and the kinetic energy density, the entropy density of pions is multiplied by d_g/d_π for comparison. We see that s_g and $s_\pi d_g/d_\pi$ have almost the same constant value during the phase transition. The average value of s_g agrees well with $s_g^c = s_g(\tau_c) = 8.3297 \text{ fm}^{-3}$, denoted by the dashed line.

After the phase transition is complete in the considered volume element, the number, energy, and entropy density, and the temperature of pions in that volume element decrease in time. The numerical results agree well with the analytical solutions (not shown).

In Fig. 6 we present the time evolution of the total number, energy, and entropy density in the mixed phase according to Eqs. (8), (9), and (25), but replacing n_g^c , n_π^c ,

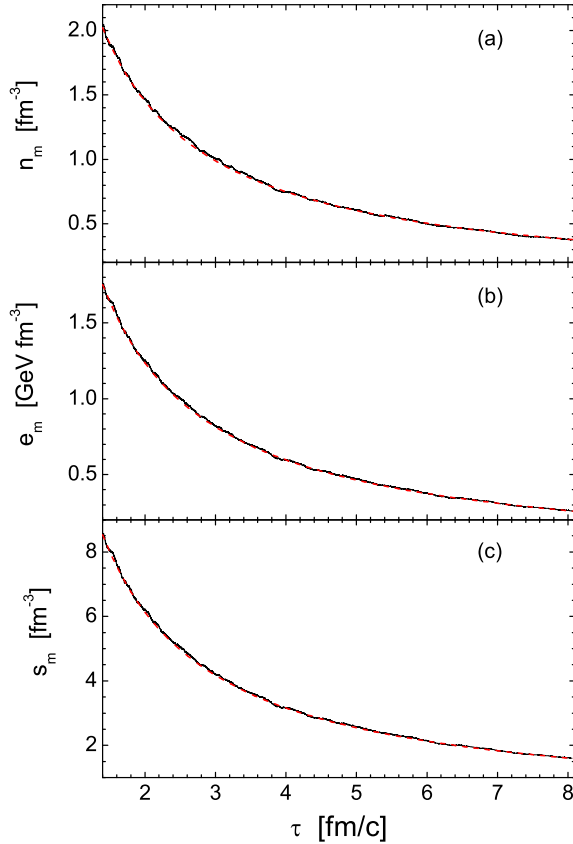


FIG. 6: (Color online) The time evolution of the total number, energy, and entropy density. The solid curves (in black) depict the numerical densities, while the dashed curves (in red) depict the analytical solutions.

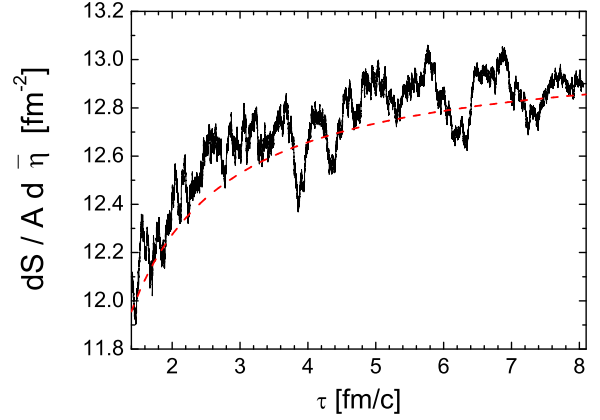


FIG. 7: (Color online) Same as Fig. 6, but for the total entropy per space-time rapidity per transverse area.

e_g^c , e_π^c , s_g^c , and s_π^c by the numerical values given in Figs. 4 and 5. Comparisons with the analytical solutions given in Eqs. (46), (47), and (44) show perfect agreements. The total entropy per space-time rapidity and per transverse area is obtained by multiplying the total entropy density by the time τ and is depicted in Fig. 7. We see that the increase of the total entropy during the hadronization is realized in our dynamical hadronization scheme and agrees well with the analytical solution.

VII. SUMMARY AND OUTLOOK

In this article we have implemented a dynamical hadronization scheme describing the first-order confinement and deconfinement phase transition between gluons and pions. The continuous change of the gluon volume and the pion volume are derived theoretically by the energy balance according to the condition of the phase equilibrium. Based on the derived volume changes, the transition probabilities of the considered microscopic processes $g+g \rightarrow \pi+\pi$, $g+g \rightarrow \pi+\pi+\pi$, and their back reactions are determined to mimic the phase transition within a kinetic transport approach. We have carried out a simulation of the phase transition in a one-dimensional expansion with Bjorken boost invariance and compared the numerical results with the analytical solutions. We have seen almost perfect agreements. This demonstrates the applicability of our dynamical scheme in describing the first-order confinement and deconfinement phase transition in a more realistic expansion of the QCD matter produced in relativistic heavy-ion collisions.

In future works we will first improve the present hadronization scheme by adding quarks and more hadron species and apply it to study the relation between the collective flow of hadrons and that of quarks and gluons. In particular, we would like to address the contribution of gluons to the collective flow of hadrons and to examine whether there is a real quark number scaling.

Second, we will investigate the dissipative effect in the distribution function of hadrons during the phase transition and quantify the difference from that obtained by using the Cooper-Frye prescription after viscous hydrodynamic calculations. Third, we will implement hadronic transport processes and establish a multiphase transport model, which is able to describe all stages of heavy-ion collisions. In addition, referring to the dynamics within the chiral σ model [38, 39] or the Nambu-Jona-Lasinio model [40, 41], we want to include both the confinement and chiral phase transition in one transport approach, where interactions between particles and fields [42] will be implemented explicitly.

Acknowledgement

ZX thanks P. Huovinen and C. M. Ko for helpful discussions. This work was financially supported by the NSFC and the MOST under Grants No. 11275103, No. 11335005, No. 11575092, and No. 2015CB856903. The BAMPS simulations were performed at Tsinghua National Laboratory for Information Science and Technology.

-
- [1] BRAHMS Collaboration, I. Arsene *et al.*, Nucl. Phys. A **757**, 1 (2005).
 - [2] B. B. Back *et al.*, Nucl. Phys. A **757**, 28 (2005).
 - [3] STAR Collaboration, J. Adams *et al.*, Nucl. Phys. A **757**, 102 (2005).
 - [4] PHENIX Collaboration, K. Adcox *et al.*, Nucl. Phys. A **757**, 184 (2005).
 - [5] ALICE Collaboration, K. Aamodt *et al.*, Phys. Rev. Lett. **105**, 252302 (2010).
 - [6] ATLAS Collaboration, G. Aad *et al.*, Phys. Rev. Lett. **105**, 252303 (2010).
 - [7] CMS Collaboration, S. Chatrchyan *et al.*, Phys. Rev. C **84**, 024906 (2011).
 - [8] Z.-W. Lin and C. M. Ko, Phys. Rev. Lett. **89**, 202302 (2002); V. Greco, C. M. Ko and P. Levai, *ibid.* **90**, 202302 (2003); R. J. Fries, B. Müller, C. Nonaka and S. A. Bass, *ibid.* **90**, 202303 (2003); D. Molnar and S. A. Voloshin, *ibid.* **91**, 092301 (2003); R. C. Hwa and C. B. Yang, Phys. Rev. C **67**, 064902 (2003).
 - [9] STAR Collaboration, B. I. Abelev *et al.*, Phys. Rev. C **77**, 054901 (2008).
 - [10] M. Luzum and P. Romatschke, Phys. Rev. C **78**, 034915 (2008); **79**, 039903(E) (2009).
 - [11] K. Dusling, G. D. Moore and D. Teaney, Phys. Rev. C **81**, 034907 (2010).
 - [12] H. Song, S. A. Bass and U. Heinz, Phys. Rev. C **83**, 024912 (2011).
 - [13] B. Schenke, S. Jeon and C. Gale, Phys. Rev. Lett. **106**, 042301 (2011).
 - [14] H. Niemi, G. S. Denicol, P. Huovinen, E. Molnar and D. H. Rischke, Phys. Rev. Lett. **106**, 212302 (2011).
 - [15] D. Molnar and Z. Wolff, arXiv:1404.7850 [nucl-th].
 - [16] F. Cooper and G. Frye, Phys. Rev. D **10**, 186 (1974).
 - [17] H. Stoecker *et al.*, J. Phys. G **43**, 015105 (2016).
 - [18] B. Svetitsky and L. G. Yaffe, Nucl. Phys. B **210**, 423 (1982); T. Celik, J. Engels and H. Satz, Phys. Lett. B **125**, 411 (1983); F. Karsch, Nucl. Phys. A **698**, 199 (2002); S. Borsanyi, G. Endrodi, Z. Fodor, S. D. Katz and K. K. Szabo, J. High Energy Phys. **1207**, 056 (2012); A. Francis, O. Kaczmarek, M. Laine, T. Neuhaus and H. Ohno, Phys. Rev. D **91**, 096002 (2015).
 - [19] Y. Aoki, Z. Fodor, S. D. Katz and K. K. Szabo, J. High Energy Phys. **0601**, 089 (2006).
 - [20] A. Bazavov *et al.*, Phys. Rev. D **80**, 014504 (2009).
 - [21] Z. Xu and C. Greiner, Phys. Rev. C **71**, 064901 (2005); Z. Xu and C. Greiner, *ibid.* **76**, 024911 (2007); J. Uphoff, F. Senzel, O. Fochler, C. Wesp, Z. Xu and C. Greiner, Phys. Rev. Lett. **114**, 112301 (2015).
 - [22] Z. W. Lin, C. M. Ko, B. A. Li, B. Zhang and S. Pal, Phys. Rev. C **72**, 064901 (2005).
 - [23] W. Cassing and E. L. Bratkovskaya, Phys. Rev. C **78**, 034919 (2008).
 - [24] A. Chodos, R. L. Jaffe, K. Johnson, C. B. Thorn and V. F. Weisskopf, Phys. Rev. D **9**, 3471 (1974).
 - [25] Z. Xu, K. Zhou, P. Zhuang and C. Greiner, Phys. Rev. Lett. **114**, 182301 (2015).
 - [26] D. H. Rischke, Y. Pursun and J. A. Maruhn, Nucl. Phys. A **595**, 383 (1995); **596**, 717(E) (1996).
 - [27] J. Sollfrank, P. Huovinen, M. Kataja, P. V. Ruuskanen, M. Prakash and R. Venugopalan, Phys. Rev. C **55**, 392 (1997).
 - [28] P. F. Kolb, J. Sollfrank and U. W. Heinz, Phys. Rev. C **62**, 054909 (2000).
 - [29] P. Chomaz, M. Colonna and J. Randrup, Phys. Rept. **389**, 263 (2004).
 - [30] J. Steinheimer and J. Randrup, Phys. Rev. Lett. **109**, 212301 (2012).
 - [31] F. Li and C. M. Ko, arXiv:1606.05012 [nucl-th].
 - [32] A. Muronga, Phys. Rev. C **69**, 034903 (2004).
 - [33] J. D. Bjorken, Phys. Rev. D **27**, 140 (1983).
 - [34] P. Huovinen and D. Molnar, Phys. Rev. C **79**, 014906 (2009).
 - [35] C. Wesp, A. El, F. Reining, Z. Xu, I. Bouras and C. Greiner, Phys. Rev. C **84**, 054911 (2011).
 - [36] A. El, F. Lauciello, C. Wesp, Z. Xu and C. Greiner, Nucl. Phys. A **925**, 150 (2014).
 - [37] A. El, Z. Xu and C. Greiner, Phys. Rev. C **81**, 041901 (2010).
 - [38] M. A. Stephanov, Phys. Rev. D **81**, 054012 (2010).
 - [39] M. Nahrgang, S. Leupold, C. Herold and M. Bleicher, Phys. Rev. C **84**, 024912 (2011).
 - [40] S. Plumari, V. Baran, M. Di Toro, G. Ferini and V. Greco, Phys. Lett. B **689**, 18 (2010).
 - [41] R. Marty and J. Aichelin, Phys. Rev. C **87**, 034912 (2013).
 - [42] C. Wesp, H. van Hees, A. Meistrenko and C. Greiner, Phys. Rev. E **91**, 043302 (2015); C. Greiner, C. Wesp, H. van Hees and A. Meistrenko, J. Phys. Conf. Ser. **636**, 012007 (2015).